Micromegas Detector Using ^{55}Fe X-ray Source

Hamid Mounir [#1], Seddik Bri* [2]

[#] Spectrometry Laboratory of Materials and Archaeomaterials (SLAMAR), Faculty of Science, Moulay Ismail University, Meknes – Morocco

[*] Electrical Engineering Department, High Scool of Technology, ESTM, Moulay Ismail *University, Meknes- Morocco*

ABSTRACT

The Multi-Wire Proportional Chamber (MWPC) and MICROMEGAS (Micro-Mesh Gas Structure) detectors are the major families of position detectors in High Energy Physics, introduced in the late sixties, detect and localize energy deposit by charged particles over large area, are widely used in particles. The goal of this work is to simulate the potential and electric field distribution in (MWPC) detector, to clarify the phenomenon of induction of signals in the electrodes of the MICROMEGAS detector, in particular, in avalanche and micro-mesh. Initially, we focus on electronic and ionic currents induced, then; we will calculate the total charge induced. We choose Argon-isobutane(Ar-iC4H10) and Argon-dimethyl-ether (DME) gas mixture, using ^{55}Fe radioactive 5.9keV X-rays source. In the normal condition, (T=298k, p=1atm), we will simulate the temporal structure of the current signal, and the contribution of the total charge induced, then we will simulate the pre-amplified signal. These results are compared to other results published. Finally, we will discuss the dependence of the output signal at the parameters of MICROMEGAS detector noting some remarks on improving the performance of MICROMEGAS.

Key words: MWPC, MICROMEGAS, Modeling and Simulation, MATLAB Program, Avalanche phenomenon, Primary Ionization, Townsend coefficients, Mixture Gas, Electric and Amplification field, Micromesh, Signal.

Corresponding Author: Hamid. Mounir.

INTRODUCTION

Initially, all detectors were traces of an optical nature, and each event was analyzed individually. Any electronic instrument was, therefore, particularly awaited. One possibility was to assemble the series of proportional tubes but this was not practical in terms of mechanics. A revolution has occurred with the invention of the Multi wires proportional chamber G. CHARPAK (WPC) [1]. Indeed, G. CHARPAK has shown that the matrix of regularly spaced wires anode in the same chamber functions as a proportional tube assembly. Moreover, with recent developments in electronics-based transistors, each thread can have its own amplifier built in the chamber. Wires chamber was quickly adopted in particle physics and stimulated new experimental generations.

The recovered signal determines the position of the interaction in a spatial coordinate. A calculation of mass center from the signals with adjacent wires may help to clarify the place of interaction. The spatial resolution of these devices is directly dependent on the spacing between the wires. For mechanical and electrostatic reasons, they cannot be reconciled; however, the

spatial resolution of this type detector was quickly capped. Despite this handicap, the MWPC has been widely exploited, because they can cover large areas at low cost. They played a major role in the development of modern detectors [2].

Gas proportional chamber based on the MICROMEGAS (MICRO Mesh Gas Structure) [3] – [4] technology is an example of a new generation of detectors that exploit narrow anode-cathode gaps, rather than thin wires, to create gas gain. These detectors are inherently pixel detectors that can be made at a large size for reasonable costs. Because of their intrinsic gain and room temperature operation, they can be instrumented at very low power per area unit, making them valuable for a variety of particle physics applications where large-area particle tracking is required.

The MICROMEGAS is a new gaseous detector initially developed for track-in high-rate, high-energy, physics experiments since 1990. It shows higher counting rate capacity up to 10^8 mm^2 s^{-1}, position-sensitive with spatial resolution better than 100 µm and good performance of radiation hardness[5]-[6], which has been developed since 1996 at Saclay, France[7]. MICROMEGAS is a Parallel Plate Detector (PPD) with three electrodes, cathode, micromesh and anode and a narrow amplification space, typically 50-100 microns, between the micromesh and the anode. The detector gain depends directly on the distance between the micromesh and anode; therefore, controlling the geometry of the amplification region is crucial in order to achieve good energy resolution [4].

The concept, developed for tracking applications, has shown great promise for handling high data rates with a rather low cost structure. The working principle is based on the double stage parallel plate avalanche chamber. MICROMEGAS is widely used in particle physics and is a suitable candidate in high-intensity X-ray detection and tomography.
In order to improve the performance of MICROMEGAS detector by optimizing some parameters, we will, therefore, study the effects of all these parameters and find compromise that allows us to operate the MICROMEGAS in conditions where it will be 100% effective for particles at least in ionization and be able to find the position of the passage of the particle with great precision. First, we will establish the basic equations that underpin our work. Our simulation model based on a numerical calculation code developed by MATLAB Program, using the gas mixture Ar-isobutane (Ar-C_4H_9) and Ar-dimethyl-ether (Ar-CH_2-O-CH_3) that decrease the diffusion coefficients, we use also, ^{55}Fe source that produces x-ray photons of 5.9KeV. The temporal evolutions of electron and ion current were simulated. The output signals of micromesh and the temporal evolution of total charge were also calculated. These results are compared with that obtained in author's literature with author gas mixture.

MODELING AND PHYSICAL PROCESS

The (MWPC) detector, shown schematically in figure 1, consists of grid of parallel wires (anodes) equidistant (the order is about one millimeter) between two cathodic plans heated to a high voltage and defining a volume filled with gas. During the passage of a charged particle, the ionization electrons produced in the gas drifted toward the anode under the effect of electric field and multiplied in their environment. An electrical pulse appears on the wire anodes. In the MWPC, the spatial resolution is closely related to the spacing between the wires anode. It is technically difficult to reduce that distance under one millimeter.

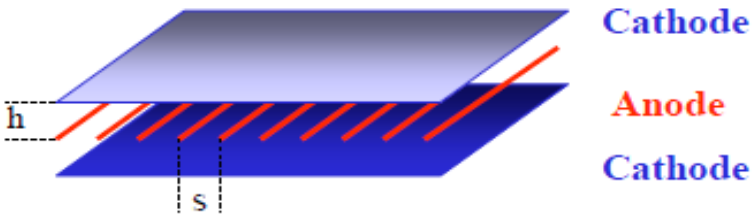

Fig 1: Diagram of multi-wire proportional chamber (MWPC) detector

The physical processes that determine the functioning of the gas detectors are statistical in nature: the ionization of gas molecules, the diffusion of free electrons, the gas amplification, etc. These statistical processes can be measured and understood, however, if all the possible functions governing the detector are known, it will be very difficult to find analytical expressions to calculate the performance of detector such as the efficiency or spatial resolution.

When many of probabilistic phenomena must be taken into account simultaneously, an alternative approach to analytical solutions is the simulation. It is a simulation on a computer, a physical phenomenon: giving an initial condition, all processes are evaluated, and if a probabilistic phenomenon comes into play in the process, then a random choice is made at the probabilistic distribution of the phenomenon in question. The interpretation of results requires great caution because predictions are based on theoretical or empirical model, the validity of which is limited. Therefore, the simulation results must be verified whenever possible by a comparison with appropriate experiences.

This is a multi-wire chamber detector characterized by the size shown on the figure below, the mathematical expression of the potential is usually calculated analytically using conformal mapping or transformation Christoffel-Schwartz [8]. The configuration that we want to study is shown in the diagram below, it is a matrix that represents a grid (wires anode) of length L, these parallel wires are placed equidistant from s=1mm including a plan inserted into a gap of thickness Δ. The dimensions characterizing the detector are shown in figure 2.

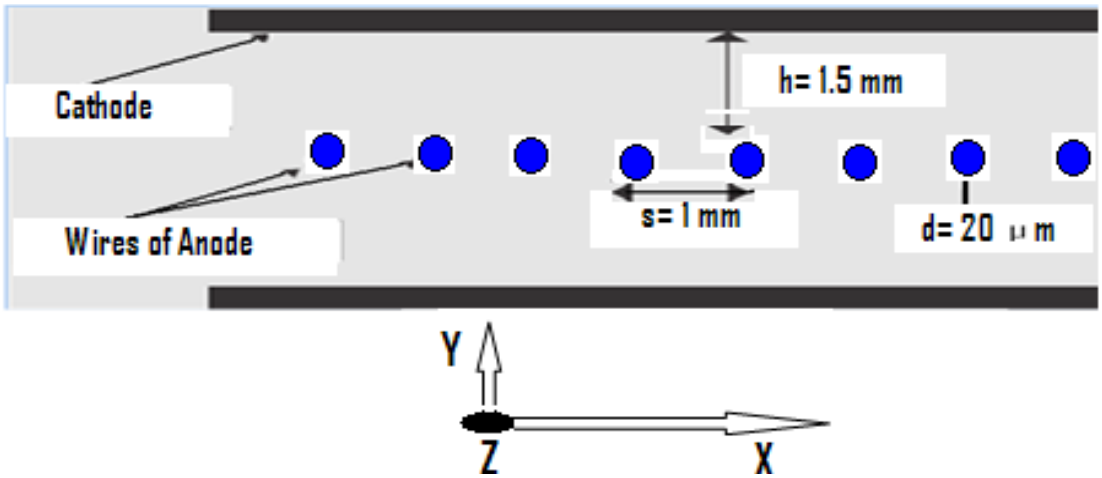

Fig 2: Front view and dimensions of (MWPC) detector

POTENTIAL AND ELECTRIC FIELD DISTRIBUTION

The distribution of potential and electric field in a multi wire proportional chamber or drift chamber can generally be calculated in good precision of the exact formula for the potential around a set of lines of charge q along the axis oz and located in: $y = 0,\ x = 0,\ \pm s, \pm 2s, \ldots\ldots$

$$V(x,y) = -\frac{q}{4\pi\varepsilon_0}\ln\left\{4\left[\sin^2\left(\frac{\pi x}{s}\right) + \sinh^2\left(\frac{\pi y}{s}\right)\right]\right\} \quad (1)$$

The profile of potential distribution is represented in the figure below, simulated by MATLAB Program

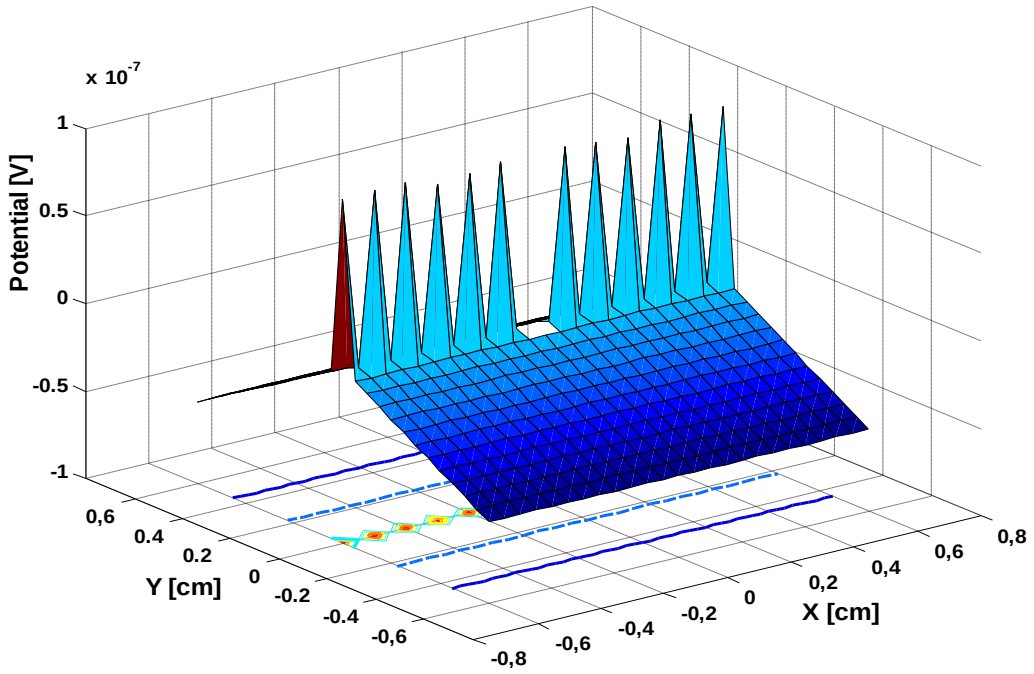

Fig 3: Potential distribution in MWPC detector

Finally, we can get the total field:

$$E(x,y) = \frac{q}{4\varepsilon_0 s}\frac{\left[\sin^2\left(\frac{2\pi x}{s}\right) + \sinh^2\left(\frac{2\pi y}{s}\right)\right]^{\frac{1}{2}}}{\sin^2\left(\frac{\pi x}{s}\right) + \sinh^2\left(\frac{\pi y}{s}\right)} \quad (2)$$

Figure 4 shows the profile of Electric Field distribution, calculated using the MATLAB Program

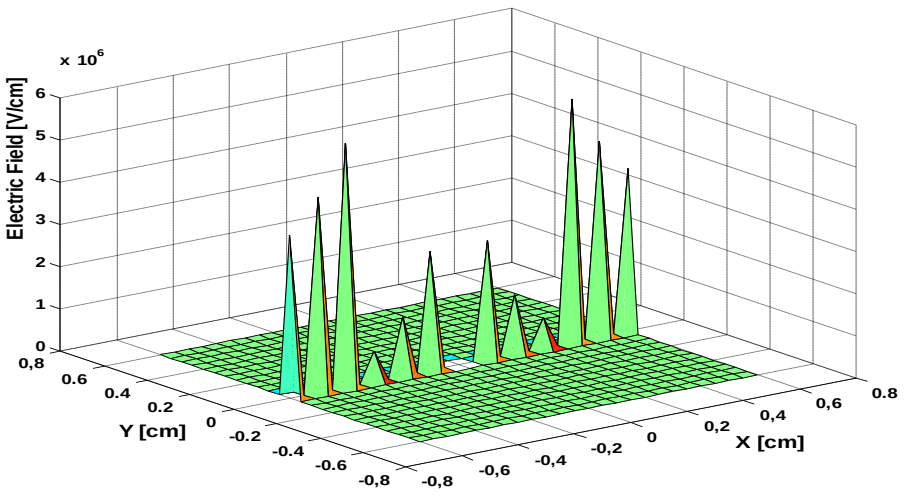

Fig 4: Electric Field distribution in MWPC detector

The equations of equipotential surfaces are

$$\cosh\left(2\frac{\pi y}{s}\right) = \cos\left(2\frac{\pi x}{s}\right) \quad (3)$$

The field lines are determined by the equation:

$$tanh\left(\frac{\pi y}{s}\right) = k\ tan\left(\frac{\pi x}{s}\right) \quad (4)$$

Where k is an integration's constant.
The profile of the field lines is shown in figure 5, calculated using the Garfield program [9].

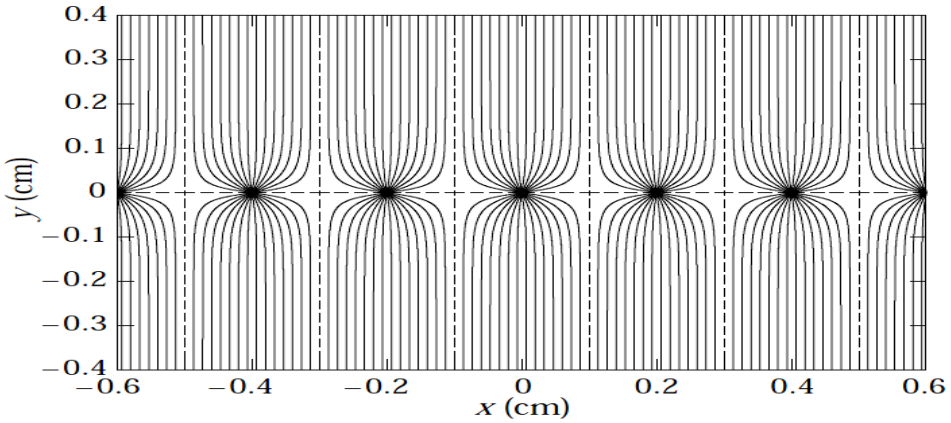

Fig 5: Field lines in a MWPC detector, calculated by Garfield Program

DESCRIPTION AND BASIC PRINCIPLE OF MICROMEGAS DETECTOR

In more recent design (1985), MICROMEGAS (Micromesh Gaseous Structure) suggests that new higher performance techniques previously developed. It operates on the principle of multi-wire proportional chamber (MWPC), but with better spatial resolution (≤ 50 microns) and a more rapid formation of the signal. MICROMEGAS is a gaseous detector strongly asymmetric parallel faces. The basic principle is to decouple the drift region of the amplification gap, either by a grid wires, but by a very fine metal grid (3 microns thick). The trick lies in the use this micromesh pierced by a multitude of holes (in less than or equal to 50µm).

MICROMEGAS principle is illustrated in figure 6. It consists of a drift gap (3 mm) and a thin amplification gap (100 µm). The properties of the electric field in two gaps have been studied by MC simulation with Garfield [9].The voltage of drift electrode and mesh is HV2 and HV1, respectively, and MICROMIGAS is operated in gas mixture of Argon-isobutane (Ar-isob) and Argon-dimethyl ether (Ar-DME), at a temperature of 300 K and a pressure of 1atm. The electric field in the amplification region is very high (≥40 kV/ cm), and the one in the conversion region is quite low. Therefore, the ratio between the electric field in the amplification gap and that in the drift gap can be tuned to large values. The MICROMEGAS is based on the planar electrodes. The drift electrode is made from 5×5 cm^2 500LPI (lines per inch) steel mesh pasted on an epoxy frame, and the same mesh is used as the amplification electrode. The drift gap is also called conversion gap because the ionization of the gas by incoming radiation occurs mainly in it. The field in the amplification gap catches the free electrons from the drift gap to forcefully accelerate them through the small amplification gap. They, then, acquire enough energy to ionize surrounding gas. The newly ionized electrons gain as well as sufficient energy to ionize the gas again and again, thus forming an avalanche and leading to a measurable electric signal on the anode and on the mesh.

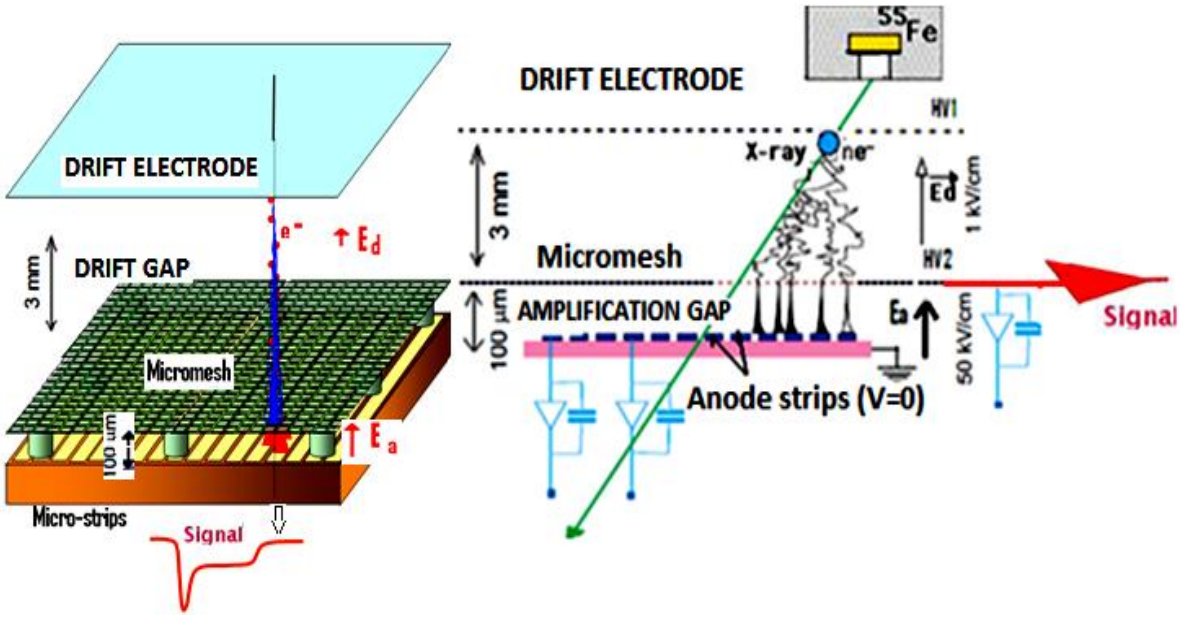

Fig 6: Schematic view of MICROMEGAS: dimensions and operating principle

Table 1 presents some parameters configuration of MICROMEGAS detector .

Table1. Parameters configuration of MICROMEGAS detector

parameter	Symbol	Example of value	Gas Mixture	Ray-source
Drift gap	h	3mm	Argon-isobutane ($Ar-C_4H_9$) Argon-dimethyl-ether **(**$Ar-CH_2-O-CH_3$)	X-ray source ^{55}Fe (5,9keV)
Amplification gap	d	100µm		
Track pitch	P_p	317µm		
Width of a track	w	250µm		
Step of the grid	P_g	52µm		
voltage drift	V_d	700V		
Voltage mesh	V_g	400V		
Drift field	E_d	$1kV.cm^{-1}$		
Amplification field	E_a	$40kV.cm^{-1}$		

ELECTRIC FIELD CONFIGURATION

A detailed description of the electric field configuration and the principle of operation are given in [10] - [11]. Ionization electrons, created by the energy deposition of an incident charged particle in the conversion gap, drift and can be transferred through the cathode micromesh; they are amplified in the small gap, between anode and cathode, under the action of electric-field, which is high in this region. The electron could is finally collected by the anode micro strips, while the positive ions are drifting in opposite direction and are collected on the micromesh. The electric-field must be uniform in both conversion and amplification spaces. This is easily obtained by using the micromesh as the middle electrode. The electric-field shape is, however, disturbed close to the holes of the micromesh. The knowledge of the shape of the field lines close to the micromesh is a fundamental issue for the operation for our detector, and especially for efficiency of the passage of electrons through the micromesh, as well as, for the fast evacuation of the positive-ion build-up.

MICROMEGAS SIGNAL

The idea of a signal obtained by charge collection in the electrodes can be confusing. Dice their appearances, the electrons and ions created the signal charges in the electrodes of the detector. For describe the formation of the signal in the detector, follow the electrons as they pass through the mesh of the micromesh and then during the avalanche. This is not the collection of charges on the electrodes, the slopes for electrons and ions to the micromesh, which is the source of the signal but it is the moving charge induces a signal in the electrodes [12].

The electron avalanche occurring in the amplification gap produces a high number of ionizations. The average of this number is called the multiplication factor or gas gain of the chamber. The

size of the avalanche shows large variations around its average value. A model of gas amplification, established in [13], gives the number of electrons n (t) in an avalanche. The current generated by the moving charges in the amplification gap has two contributions:
- A brief and fast signal due to the electrons generated mostly close to the anode plan and quickly collected (1–2 ns). The drift velocity of electron in gas is of several cmμs−1
- A long signal due to the ions moving slowly towards the mesh (100–200 ns), their drift velocity is at least two order of magnitude lower than the electrons' one.

Basic Equations

Consider the movement of n_0 electrons from the micro-grid to the anodes. Where t_e is the time of the electrons collection

$$t_e = \frac{d}{v_-} \tag{5}$$

Where d is the width of the amplification gap and *v- is* electrons velocity, we observe a current:

$$I_e(t) = \frac{n_0 q}{t_e} \quad , \quad 0 \le t \le t_e \tag{6}$$

We follow the development of the avalanche and the increasing number of electrons, we obtain:

$$I_e(t) = \frac{n_e(t) q}{t_e} \quad , \quad 0 \le t \le t_e \tag{7}$$

The number of electrons in the avalanche follows the law:

$$n_e(t) = n_0 \exp(T_w v_- t) \tag{8}$$

Where T_w is the First Townsend coefficient (amplification factor) is expressed as:

$$T_w = p\, A \exp\left(-B \frac{p}{E}\right) \tag{9}$$

Where p is the atmospheric pressure, E the amplification field and A, B are parameters of the gas mixture [5, 14, 15].

$$I_e(t) = \frac{n_0 q}{t_e} \exp\left(T_w \frac{d}{t_e} t\right), \quad 0 \le t \le t_e \tag{10}$$

The ions produced during the avalanche on vast majority, will move towards the micro-mesh with a velocity v_+ much lower than the velocity of the electrons. The ionic current will be in two

terms, the number of ions created by the development of the avalanche decreased by the number of ions that have been collected in the micromesh. The ion current is expressed thus, if v_+ is less than v_-:

$$I_{ion}(t) = \begin{cases} \frac{n_0 q}{t_{ion}}\left(\exp\left(T_w \frac{d}{t_e} t\right) - \exp\left(T_w \frac{d}{t_{ion}} t\right)\right), & 0 \le t \le t_e \\ \frac{n_0 q}{t_{ion}}\left(\exp(T_w d) - \exp\left(T_w \frac{d}{t_{ion}} t\right)\right), & t_e \le t \le t_e + t_{ion} \end{cases} \quad (11)$$

The time of ions collection is as:

$$t_{ion} = \frac{d}{v_+} \quad (12)$$

Deducting the total current in avalanche as:

$$I(t) = \begin{cases} \frac{n_0 q}{t_e} \exp\left(T_w \frac{d}{t_e} t\right) + \frac{n_0 q}{t_{ion}}\left(\exp\left(T_w \frac{d}{t_e} t\right) - \exp\left(T_w \frac{d}{t_{ion}} t\right)\right), & 0 \le t \le t_e \\ \frac{n_0 q}{t_{ion}}\left(\exp(T_w d) - \exp\left(T_w \frac{d}{t_{ion}} t\right)\right), & t_e \le t \le t_e + t_{ion} \end{cases} \quad (13)$$

From equation (13), we can deduce the total charge collected in avalanche:

$$Q(t) = \begin{cases} \frac{n_0 q}{T_w d}\left(exp\left(T_w \frac{d}{t_e} t\right) - 1\right), & 0 \le t \le t_e \\ \frac{n_0 q}{t_{ion}} exp(T_w d)\, t, & t_e \le t \le t_{ion} \end{cases} \quad (14)$$

We see that the ratio of the signals produced by electrons and ions is in the report of 1/ (T_w d), this is the movement of ions representing the main contribution of the signal over the detector.

Simulation Model

The analytical study of our system leads us to extract some equations that lead us to model our detector described above. The simulation model of the physical processes occurring within MICROMEGAS is based on the MATLAB Program that is the tool of simulation, and more effective for our work. In the general case, There are three types of parameters affecting the detector: the parameters related to the chamber (geometry), the gas parameters (diffusion, gain, Mixing coefficients), the parameters of the trace (angle, energy, signal, type of particles). From equations (9) and (13), using the table II shown below [15], we can estimate accumulated signal in the avalanche for different proportions of each gas mixture used; the same program remains what we need to change are the values of the coefficients A_i and B_i [14] – [15]. These parameters are adjusted by experience.

Table2. Gain and First Townsend coefficient for different mixtures of an amplification gap of 100 µ m wide

Mixture	Percentage	A_i (cm^{-1})	B_i ($kv.cm^{-1}$)	T_{Wi} (cm^{-1})	Amplification Gain(G_i)
Ar-isobutane	06	4700	062.70	13.4120	6.679510^5
	10	4600	069.20	11.5264	1.013610^5
	20	5700	093.90	08.7150	6.093910^3
	30	7200	119.80	06.5579	7.047710^2
Ar-DME	05	2900	039.60	13.1352	5.064610^5
	10	3100	044.40	12.7558	3.465610^5
	15	3500	052.90	12.1502	1.891410^5
	20	3300	053.60	11.2967	8.055310^4
	30	4200	069.10	10.5452	3.799410^4

The calculated results of the First Townsend coefficients (T_{wi}, i=1, 2, 3, 4, 5) and the amplification gains (G_i, i =1, 2, 3, 4, 5) for different proportions of gaseous mixtures using equation (9) and n_0=1, are obtained in [16], but in this work, we set the electric field amplification at 50 KV / cm, and see the simulated values for different proportions of the mixture in Table II above. t_e are in the order of nanoseconds and t_{ion} of the order of hundreds of nanoseconds [17].

The Global Signal Simulation in the Micromesh

The total signal is collected in avalanche calculated using the equation (13), and by applying the same calculation procedures. Figure 7 shows the results obtained.

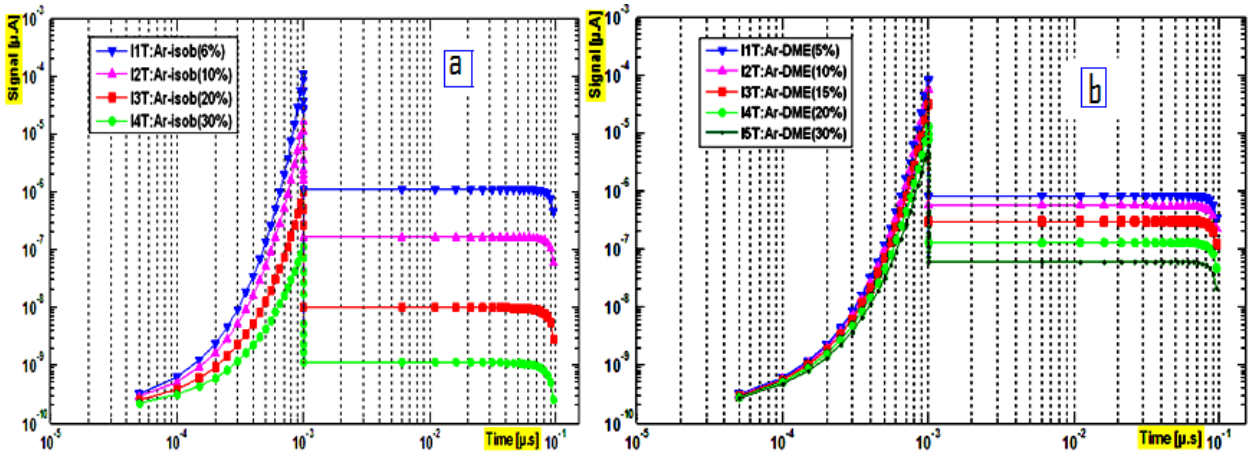

Fig7: Global Signal in avalanche for different proportions of Argon-isobutane (a) and for Argon-DME (b)

We can see the shape of the calculated total signal MICROMEGAS for both gas mixtures. Also, we note the very high speed collection of ions in MICROMEGAS. An important finding in this simulation is that the ratio of electron and ion currents in the order of the ratio of electrons and ions drift velocities.

Simulation of Charges collected in Micromesh

Equation (14) allows us to calculate all the charges collected in micro-mesh for both Ar-isobutane and Ar-DME gas mixtures following the same procedures as those applied in the simulation of the current signals. The results are shown in Figure 8

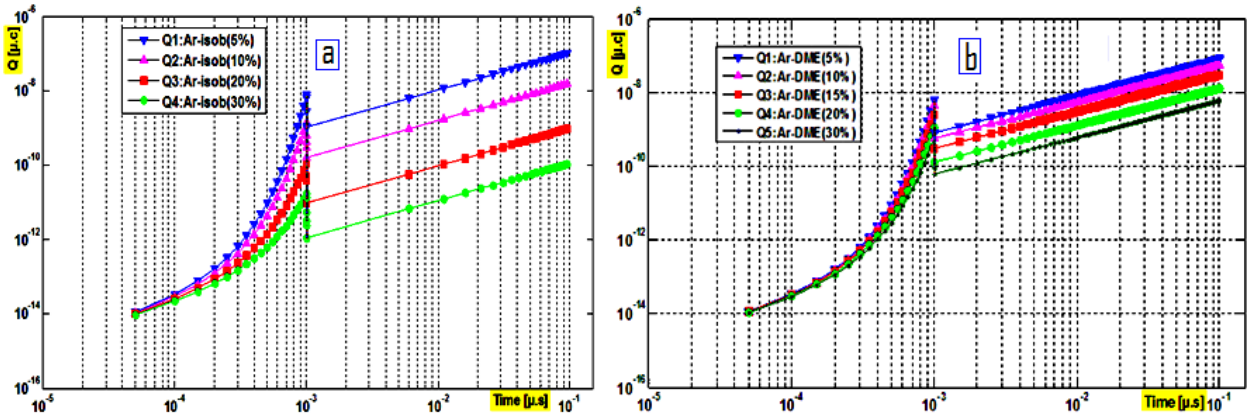

Fig8: Global charge in Micromesh for different proportions of Argon-isobutane (a) and for Argon-DME (b)

First, we note that the temporal evolution of the total charge for both gas mixtures keeps the same evolution qualitatively. On the other hand, the charge decreases with the increase in the proportion of the quencher, and that the variation for Ar-isobutane is greater than that of Ar-DME. It is interesting to note that the total charge is simply the gain multiplied by the primary charge, and that in fact the amplified electrons do not contribute much to the final detected charge. The main contribution is clearly due to ions [18].

The proportion between the two contributions relates directly to the gain of the chamber. The fraction f_e of the signal due to electrons is given by:

$$f_e = \frac{Q_e}{Q_T} = \frac{1}{T_w d}(1 - e^{-T_w d}) = \frac{1}{\text{Log}(G)} \qquad (15a)$$

Similarly we can calculate the proportion of charge induced by ions:

$$f_{ion} = 1 - f_e = 1 - \frac{1}{T_w d}(1 - e^{-T_w d}) \qquad (15b)$$

Where Q_e, is the charged induced by electrons, Q_T, the total induced charge, T_w, the first Townsend coefficient, d the gap width and G the gas gain.

The Amplification Signal

After This simulation and its results, we conclude that our MICROMEGAS is equivalent to a current generator low signal [17]. That is why; we need an amplification device to be able to clarify the quantitative calculus. Figure 9 shows the block equivalency MICROMEGAS connects to an amplifier. Where I_D (t) represents the total current calculated (equation (13)), C_D is the equivalent capacitance between the micro-mesh and the electrodes. R And C are respectively the

capacitor (depends on the length of the tracks of the detector and the surface of the grid) and the discharge resistor of the signal integrator which these values that are adjusted depending on the type of the preamplifier used (ORTEC 142A, 142B ORTEC, ORTEC 142C …). Our simulation requires values to have remarkable results acceptable and meaningful, we used an ORTEC 142A preamplifier which gives us the value of C belongs to (0pF, 30pF), and the discharge time τ = RC.

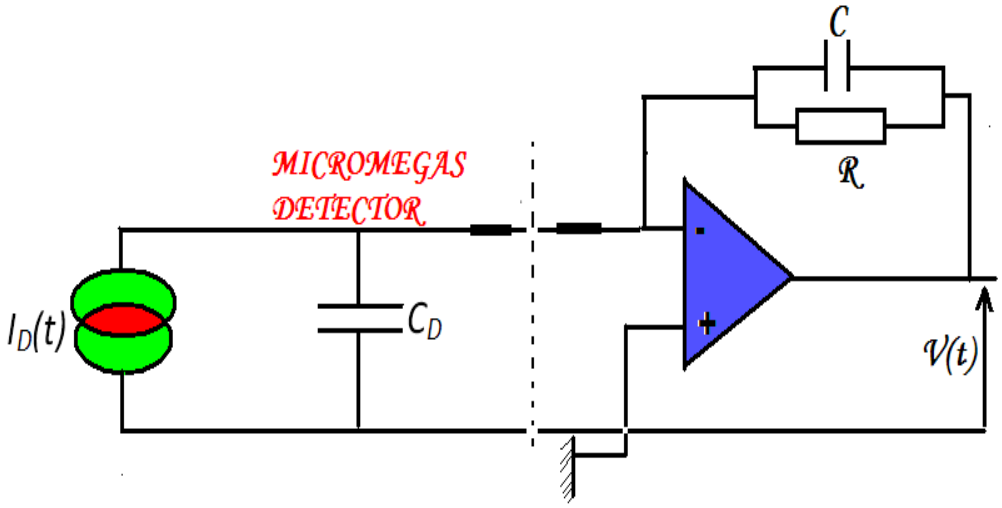

Fig9: Equivalent circuit of the MICROMEGAS detector connected to the preamplifier

The signal obtained after amplification is calculated using the above mounting and the various equations that contribute to the evolution of the signal *v (t)*, the global formula of the signal is:

$$v(t) = -\frac{n_0 q}{C}\begin{cases}\left(\frac{1}{dT_W+\frac{t_e}{\tau}}+\frac{1}{dT_W\frac{t_{ion}}{t_e}+\frac{t_{ion}}{\tau}}\right)\exp\left(T_w\frac{d}{t_e}t\right)-\frac{1}{dT_W+\frac{t_{ion}}{\tau}}\left(\exp\left(-\frac{t}{\tau}\right)-\exp\left(T_w\frac{d}{t_{ion}}t\right)\right)+\frac{1}{dT_W+\frac{t_e}{\tau}}\exp\left(-\frac{t}{\tau}\right), & 0\le t\le t_e<0\\ \frac{\tau}{t_{ion}}\exp(T_w d)\frac{1}{d.T_w}\left(1-\exp\left(\frac{t_e-t}{\tau}\right)\right)+\frac{1}{dT_W+\frac{t_{ion}}{\tau}}\left(\left(\exp(T_w\frac{d}{t_{ion}}+\frac{1}{\tau})t_e\right).\exp\left(-\frac{t}{\tau}\right)-\exp\left(T_w\frac{d}{t_{ion}}t\right)\right), & t_e\le t\le t_e+t_{ion}\end{cases} \quad (16)$$

The simulation of this parameter allows us to do best in the Functioning of MICROMEGAS and improving its performance most responding to system and puts it in a privileged state, in particular, the two main parameters: the spatial and temporal resolution. For this work, we apply the same procedures that we have seen in the temporal current simulation and that of the charge collected in the micro-mesh taking into account all parameters and gas mixtures reported above based on the tables 1, 2 and equation (16). We consider v_i (t) (i = 1, 2, 3, 4) and v_j (t) (j = 1, 2, 3, 4.5) the signals obtained after amplification in micromesh, where each index i corresponds to the percentage of the gas mixture Ar-isobutane (6, 10, 20, 30)%, and each index j corresponds to the proportions of those of Ar-DME (6, 10, 15, 20, 30)%. The results-based Ar-isobutane and those of Ar-DME are shown in Figure 10.

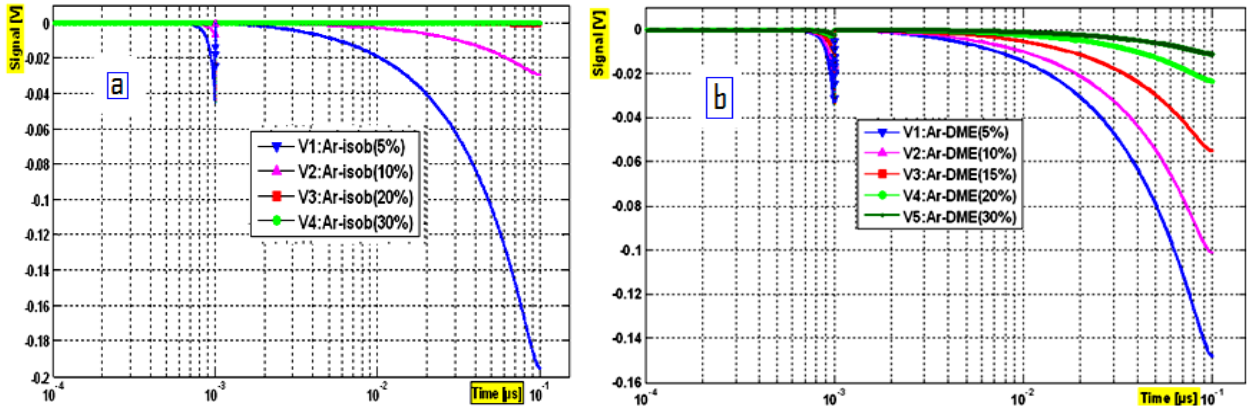

Fig10: Preamplifier output signal of MICROMEGAS for different proportions of Ar-isobutane(a) and Ar-DME(b)

The Figures Ar-isobutane (a) and Ar-DME (b) represent the evolution of the preamplifier signal in a logarithmic scale to better clarify the evolution of the signal for each percentage of the gas mixture and to facilitate the interpretation of temporal variations to recover remarks accomplished during this simulation.

CONCLUSION

In sum up, the charge induced by the electrons is much larger for MICOMEGAS that in the case of a multi-wire proportional chamber (MWPC). This property is related to the shape of the electric field. Indeed, in (MWPC), the electric field varies as (1 / r). The majority of electron-ion pairs are produced close to the fils.les electrons travel a short distance before being collected by the anode and the charge induced by the electrons is a very small fraction of the total charge. In the case of MICROMEGAS, the avalanche starts much closer to the cathode due to the uniform electric field in the amplification gap. This property allows MICROMEGAS to obtain faster and more intense signals.

In this paper, the simulated results of the MICROMEGAS detector developed are presented. The results indicate that our system with a micro-mesh (500LPI) can reach rather good operational states. However, using ^{55}Fe radioactive 5.9 keV X-rays source in an Ar-isobutane (%) and Ar-DME (%) gas mixture in normal condition. All the simulated results obtained indicate that the performances of the detector depend on many parameters, which need to be optimized for a particular purpose.

In the summary, the simulation results are nearly consistent with the data that are published in other references, and provide important information in the MICROMEGAS design, making and operation. Our simulation predicts that further improvements are still possible. We expect the use of a 500LPI would give a best spatial and temporal resolution for MICROMEGAS detector.

REFERENCE

[1] G Charpak and al. The Use of Multiwire Proportional Counters to Select and Localize Charged Particles. Nucl.Instr. and Meth. A62, P235, 1968.

[2] Roger Fourme. Position-sensitive gas detectors: MWPCs and their gifted descendants. Nucl. Instruments and Methods in Phys. Res. A392:1-11, 1997.

[3] Y. Giomataris et al. Nuclear Instruments and Method, A376, 29, 1996.

[4] Y. Giomataris, Development and prospects of the new Gaseous detector 'MICROMEGAS', Nucl. Instrum Meth. A419, 239, 1998.

[5] Sauli F. Nucl. Instrum. Methods. A 477, 1-7, 2002

[6] G. Charpak et al. Nucl. Instrum. Methods, A412, 47-60, 1998.

[7] Giomatarisa Y et al. Nucl. Instrum. Methods. A376, 29-35, 1996.

[8] E. Durand, Electrostatic, Tome 2, Paris Masson (1963).

[9] R. Veenhof, GARFIELD program: simulation of gaseous detectors, version 6.32, CERN Program Library Pool W999 (W5050). Transport Equation, Nucl. Instr. and Meth. 273, 533-535, 1975.

[10] S. A. Korff, Electrons and Nuclear Counters, Van Nostrand, Princeton (1955).

[11] D. Mazed and M. Baaliouamer. A semi-microscopic derivation of gas gain formula for Proportional Counters.Nucl. Instr. and Meth. In Phys. Res. A437: 381-392, 1999.

[12] A. Zastawny. Standardization of gas amplification, description in proportional Counters. Nucl. Instr. And Meth. In Phys. Res, A385, 239-242, 1997.

[13] Irene Peres: Kinetic modeling of electron and ion in the cylindrical proportional counters. PhD thesis, PAUL SABATIER University, TOULOUSE (1990).

[14] A. Sharma et F. Sauli, Nuclear Instruments and Methods, A334, 420-424, 1993.

[15] M. PUIL Geal: Development of Micromegas, a new gas detector for position micromesh. PhD thesis, University of Caen. (2000).

[16] H. Mounir, M. Haddad, S. Bri, International Journal of Science and Advanced Technology A 305, 89–96, 2011.

[17] Nuclear Instruments and Methods in Physics Research, A572, 999–1003, 2007.